AAPS PharmSciTech (2023) 24:51
https://doi.org/10.1208/s12249-023-02511-0

RESEARCH ARTICLE

Advancements in Amorphous Solid Dispersions to Improve Bioavailability

Preparation of Free-Flowing Spray-Dried Amorphous Composites Using Neusilin®

Zhixing Lin[1] · Kai Zheng[1] · Mohammad A. Azad[2] · Rajesh N. Davé[1]

Received: 31 August 2022 / Accepted: 10 January 2023 / Published online: 26 January 2023
© The Author(s), under exclusive licence to American Association of Pharmaceutical Scientists 2023

Abstract

A highly porous additive, Neusilin®, with high adsorption capability is investigated to improve bulk properties, hence processability of spray-dried amorphous solid dispersions (ASDs). Griseofulvin (GF) is applied as a model BCS class 2 drug in ASDs. Two grades of Neusilin®, US2 (coarser) and UFL2 (finer), were used as additives to produce spray-dried amorphous composite (AC) powders, and their performance was compared with the resulting ASDs without added Neusilin®. The resulting AC powders that included Neusilin® had greatly enhanced flowability (flow function coefficient (FFC) > 10) comparable to larger particles (100 µm) yet had finer particle size (< 50 µm), hence retaining the advantage of fast dissolution rate of finer sizes. Dissolution results demonstrated that achieved GF supersaturation for AC powders with Neusilin® was as high as 3 times that of crystalline GF concentration and was achieved within 30 min. In addition, 80% of drug was released within 4 min. The flowability improvement for AC powders with Neusilin® was more significant as compared to spray-dried ASDs without Neusilin®. Thus, the role of Neusilin® in flowability improvement was evident, considering that spray-dried AC with Neusilin® UFL2 has higher FFC than ASDs having a similar size. Lastly, the AC powders retained a fully amorphous state of GF after 3-month ambient storage. The overall results conveyed that the improved flowability and dissolution rate could outweigh the loss of drug loading resulted by addition of Neusilin®.

Keywords Amorphous composite · Amorphous solid dispersions · Flowability · Neusilin® · Spray drying

Introduction

Approximately 40% of marketed active pharmaceutical ingredients (APIs) and 80% of pharmacological compounds under development are classified as poorly water-soluble, and fall into either class 2 or 4 of the Biopharmaceutics Classification System (BCS), of which class 4 also has poor intestinal permeability [1–4]. Poor solubility of newly discovered APIs is a major hurdle in designing and manufacturing effective dosages and a lot of academic and industry efforts have gone into utilizing practical formulation/processing procedures to improve the solubility of poorly water-soluble APIs [5–10]. There are two major approaches to increase API solubility: (i) the size reduction of crystalline forms to increase the surface area and (ii) the creation of amorphous drug forms to achieve saturation solubility enhancement [9, 11–16]. Reducing particle size results in fine API with increased total surface area, improving the dissolution rate, but it fails to enhance drug supersaturation, which is needed for drugs with a water solubility < 50 mg/mL [17]. Excessive agglomeration is another problem with fine APIs that in most cases, nullifies the expected advantage of micronization to achieve faster dissolution rates [18]. In addition, fine APIs (e.g., median particle size less than 20 µm) are highly cohesive with poor flowability due to strong interparticle force [9, 19–22]. Consequently, pharmaceutical blends with poor flowing APIs have processing problems at high API doses or poor content uniformity at low API doses [23]. Owing to such limitations, amorphous drug forms are of increased interest; in particular, finer sized amorphous solid dispersion (ASD) powders with good flowability are highly desired [24].

✉ Rajesh N. Davé
dave@njit.edu

[1] New Jersey Center for Engineered Particulates, New Jersey Institute of Technology, Newark, NJ 07102, USA

[2] Chemical, Biological and Bioengineering Department, North Carolina A&T State University, Greensboro, NC 27411, USA

Solvent evaporation and melting are the two main techniques employed to create amorphous drug forms [24]. Drug degradation caused by high temperatures is the main disadvantage of melting processes, while solvent evaporation methods would be preferred to avoid degradation because organic solvent evaporation can be done at low temperatures [25]. Spray drying is one of the most popular solvent evaporation methods [26]. While it has several advantages such as preferred suitability to both heat-sensitive and heat-resistant APIs, the capability for continuous processing, and achieving consistent powder quality throughout a well-designed drying process [27], it has a high environmental footprint and low yield rate [28–31]. Additionally, spray drying poses certain constraints such as avoiding high viscosity for the solution and propensity for nozzle clogging during atomization [28, 32, 33]. Furthermore, developing a proper formulation for spray drying presents challenges, such as overcoming any potential drug and carrier polymer miscibility issues, maintaining the metastable state after spray drying, and a lack of adequate predictive models to guide formulation development [34]. Last, as is well-known, ASDs may also have low bulk density, which may be a drawback for downstream processing [32]. However, it can produce particles as fine as micron-size within a very short time [25, 35]. Before spray drying, the drug substance and carrier(s) are both dissolved in common solvents or solvent mixtures during the solvent evaporation process. The solvent removal by spray drying can lead to a very fine sized molecular mixture of drug and carrier(s), called amorphous solid dispersions (ASDs) [10, 36]. Fine sized ASDs hold significant promise to enhance drug solubility, thus dissolution performance of APIs by converting APIs' state from crystalline to amorphous [9]. Unfortunately, finer sized ASDs have a higher tendency to recrystallize due to their decreased size and increased specific surface area, leading to API recrystallization and precipitation, hence decreasing the supersaturation [10]. Although finer ASDs can contribute to faster drug release, their poor flowability is a major problem. Several groups have reported that producing larger sized ASDs using spray drying may be beneficial for the purpose of improving flowability. For example, larger scale production using large-scale spray dryers could produce larger sized, more spherical, and denser particles, beneficial from flowability perspective [37, 38]. Other reports also show various ways to achieve increased particle size [39, 40]. However, larger size usually comes with certain disadvantages such as slower dissolution rates [41] or weaker tablet tensile strength [39]. There are a few examples where adding materials like leucine, which separates out to form a coating layer on the surface of the spray-dried particle, hence achieves surface-modified powders with improved flowability [42, 43]. However, such reports have not reported dissolution profiles and were targeting inhalation applications. The issue of flowability is not necessarily limited to spray drying and challenges can be seen with milled hot-melt extrusion (HME) extrudates. It has been reported that in general, larger milled particles were more desirable to achieve very good flowability, but those may have slower dissolution rates [44–46]. Overall, achieving better powder flowability from either spray-dried or HME-produced materials without attaining larger particle sizes remains a challenge.

One potential approach to alleviate the flowability problem for spray-dried powders is the addition of highly porous functional carrier(s), which could not only contribute to forming stable ASDs with faster, higher levels of drug dissolution, but also achieve higher drug load and improved flowability. However, such additives also decrease the drug loading; hence, judicious selection of their amounts remains challenging due to the need for maintaining higher drug loading as well as a higher stability of the ASDs [47]. Ideally, the stabilizing carrier(s) should increase the flowability and packability of the solid dispersion as well as contribute to higher drug release [42, 48, 49]. However, some additives could only work as precipitation inhibitors or supersaturation maintainers [50, 51], while some could only enhance flowability and processability [48]. Neusilin® is one of the possible carriers as a high function stabilizer, a precipitation inhibitor, and a flow enhancer [48, 52–55]. Neusilin® is defined as magnesium aluminometasilicate ($Al_2O_3MgO_{1.7}SiO_2 \cdot \times H_2O$), a fine synthetic amorphous powder with high porosity and adsorption ability. Its enormous specific surface area makes it an excellent adsorption core material. It may also prevent amorphous pharmaceuticals from recrystallizing owing to nano-confinement of the drug-Neusilin® complex formation caused by the acid–base reaction, hydrogen bonding effect, and ion–dipole interactions [55–60]. Several studies have shown its remarkable capacity to improve supersaturation while obtaining excellent stability at high drug loading [55, 56, 61]. Another study showed that due to the large specific surface area and adsorption capacity of Neusilin®, the co-melt of API and surfactant was adsorbed onto it via hot-melt granulation [48]. The surface area of the API was increased by forming ASD granules, resulting in a higher dissolution rate. Meanwhile, the decreased angle of repose and increased bulk density implied enhanced flowability and tabletability, respectively. Hence, Neusilin® could be used as a potential flow enhancer for ASDs.

The main objective of this work is the generation of drug-containing particles with improved flowability and bioavailability by using Neusilin® as a minor component within the amorphous composites (ACs). A BCS (Biopharmaceutics Classification System) class 2 drug, griseofulvin (GF), was used as a model drug. AC formulation containing Soluplus-surfactant (SDS: sodium dodecyl sulfate) [25] with Neusilin® was investigated to form fine spray-dried powders that could

achieve enhanced solubility, stability, and flowability [25, 62]. Soluplus is widely used in ASDs of poorly soluble drugs [10, 25, 63–66]. It has a glass transition temperature of 70 °C, and it permits the low drying temperature to prepare ASDs. Low drying temperatures contribute to spherical particle formation [67]. SDS as a minor component can improve ASD's wettability, enabling faster supersaturation [62]. Laser diffraction was used to measure the particle size of the spray-dried powders, X-ray powder diffraction (XRPD) was used to assess the solid state of GF in spray-dried powders, the Freeman Technology FT4 powder tester was used to evaluate the AC powder flowability and bulk density, scanning electron microscopy (SEM) was used to obtain spray-dried powder images, and the USP II dissolution apparatus with UV spectroscopy was used to analyze drug release behavior of the spray-dried powders.

Materials and Methods

Materials

BP/EP-grade micronized griseofulvin (G; d_{50}: 11 µm) was provided by Letco Medical (Decatur, AL, USA). Soluplus (Sol) was donated by BASF (Tarrytown, NY) and used as a stabilizer. Sodium dodecyl sulfate (SDS) was purchased from GFS Chemicals, Inc. (Columbus, OH) and used as a surfactant in ASDs. Acetone (ACS reagent, 99.5 percent) was purchased from BDH Analytical Chemicals (VWR, GA) and employed as a solvent. Neusilin® powders, UFL2 and US2, were donated by Fuji Chemicals (Burlington, NJ), having d_{50} sizes of 3 and 105 µm, respectively.

Preparation of GF ASDs and AC via Spray Drying

GF solution or slurry feeds were prepared for spray-dried ASDs and AC, respectively (see Fig. 1). GF was employed as a model BCS Class II drug, since it is recognized as fast recrystallization drug [68]. The solubility of GF in deionized (DI) water at 25 °C and 37 °C are 8.9 mg/L and 14.2 mg/L, respectively [68]. The GF amorphous solubility varies from 28 to 38 mg/L [9, 25, 69, 70]. GF slurry containing Neusilin® was used to prepare spray-dried AC, while GF solution without Neusilin® was used to prepare spray-dried ASDs. The formulations used in this study are presented in Table I. The drug loading was theoretically calculated as the drug weight fraction in the final spray-dried powder. A solvent combination of 20 mL DI water added to 100 mL acetone was prepared. A magnetic stirrer was utilized during solution/slurry preparation. After the polymer and surfactant dissolved in the binary solvent, GF was added to the solution. When GF dissolved, the solutions were sonicated for 10 min. Neusilin® was then added to the solution under sonication for additional 20 min to prepare the slurry feed for spray-dried AC preparation. Solution feed without Neusilin® was directly fed into spray drier after sonication for ASD

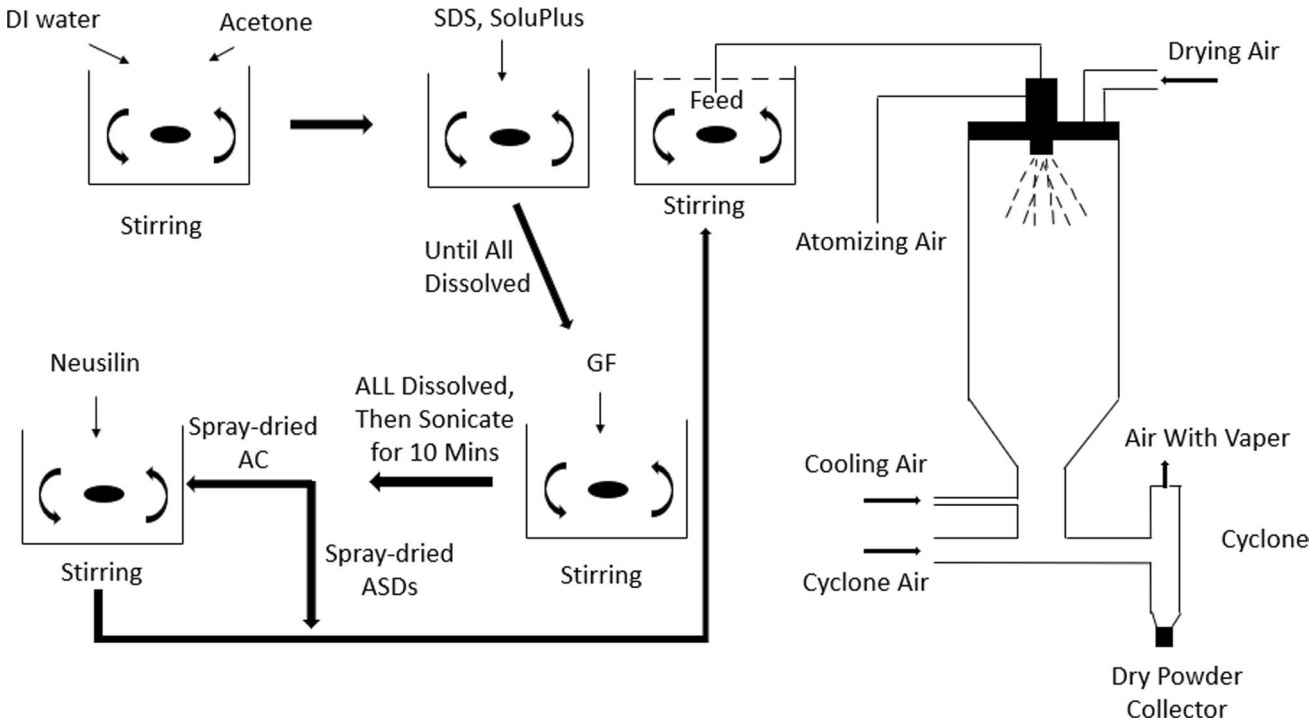

Fig. 1 Schematic of sample preparation and spray drying process

Table I Formulations Used for This Study and Theoretical Drug Loading of Each Sample

Sample no	GF:Soluplus:Neusilin®	GF (g)	SDS (g)	DI water (mL)	Acetone (mL)	Soluplus (g)	Neusilin® (g)	Neusilin® type	Theoretical drug loading (%)
1	3:6:0	3	0.15	20	100	6	-	-	32.8
2	3:3:3	3	0.15	20	100	3	3	UFL2	32.8
3	3:6:3	3	0.15	20	100	6	3	UFL2	24.7
4	3:9:3	3	0.15	20	100	9	3	UFL2	19.8
5	3:6:2	3	0.15	20	100	6	2	UFL2	26.9
6	3:6:3	3	0.15	20	100	6	3	US2	24.7

Table II Spray Dryer Operation Parameters

Parameters	Value
Liquid (solution or slurry) feed rate	1.6 g/min
Atomizing air flow rate	202.7 L/min
Drying air temperature	75 °C
Drying air flow rate	0.3 m^3/min
Atomization pressure	2 bar
Nozzle tip diameter	0.2 mm

preparation. During the preparation of feeds, a shear mixer from Fisher Scientific Laboratory Stirrer (Catalog No. 14–503, Pittsburgh, PA) was used to mix the solvent and powder except for the sonication step.

GF solution or slurry feed was dried in a spray dryer (4M8-Trix, Procept, Zelzate, Belgium), and the schematic of the drying process is shown in Fig. 1. The spray dryer's overall length and diameter are 1.59 m and 0.15 m, respectively. Drying air (75 °C) was fed from the top of the drier column at a 0.3-m^3/min flow rate (see Table II for spray dryer operation parameters). A peristaltic pump (Make-it-EZ, Creates, Zelzate, Belgium) was used to pump and spray 200 g solution or slurry (approximately 2 batches of GF-Polymer solution or suspension) into the spray dryer at a rate of 1.6 g/min. The dried particles were separated from the outflow stream into a glass jar using a cyclone separator. An atomizing air pressure at 2 bar, a bi-fluidic nozzle with a tip diameter of 0.2 mm, and a cyclone pressure of 55–60 mbar were chosen. The spray drying condition was selected based on the previous work [25]. The spray-dried powder was collected from the collection jar and then transferred into a plastic bag. The bags were stored in a vacuum desiccator at room temperature.

Particle Size Analysis Using HELOS/RODOS Particle Sizer

A Sympatec HELOS/RODOS laser diffraction particle size analyzer (Sympatec Inc., Pennington, NJ) was used to examine the particle size distributions. Approximately 1.5 g of powder (as-received GF, as-received Neusilin® UFL2 and US2, spray-dried ASDs, or AC) was dispersed into a dry dispersion feeder system, and particle size distribution was tested under 1-bar dispersion pressure. Table III shows the d_{10}, d_{50}, and d_{90} of the particle size calculated by Sympatec WINDOX 5.0 software. Previous literature details the measurements using the HELOS/RODOS laser diffraction particle size analyzer [52, 71].

X-ray Powder Diffraction

X-ray powder diffraction (XRPD) was performed using Empyrean Series 2 X-ray diffraction machine (Westborough,

Table III Properties of As-Received GF and Different Formulated Spray-Dried Composites

Sample no	Description	Status (measured by XRPD)	d_{10} (μm)	d_{50} (μm)	d_{90} (μm)	Flow function coefficient (FFC)	Bulk density (BD) (g/mL)
-	As-received GF	Crystalline	3	11	21	3.16	0.266
-	As-received Neusilin® UFL2	Amorphous	1	3	10	-	-
-	As-received Neusilin® US2	Amorphous	32	110	189	-	-
1	Spray-dried ASDs	Amorphous	6	19	37	7.35	0.461
3	Spray-dried composites with Neusilin® UFL2	Amorphous	8	19	38	> 10	0.299
6	Spray-dried composites with Neusilin® US2	Amorphous	13	36	65	> 10	0.393

MA, USA) to examine the samples of as-received GF, spray-dried ASDs, or AC. The diffractometer with a Cu Kα radiation source ($\lambda = 1.5418740$ Å) was set as 45 kV and 40 mA. The divergence slit, receiving slit, and detector slit were 2°, 10°, and 10°, respectively. Step time was 10.2 s per step, and patterns were recorded between 5° and 50°. The sample volume required for XRPD was about 0.3 cm^3. The XRPD analysis was performed after 3–6 months of storage.

Field Emission Scanning Electronic Microscope

Small amounts of powder samples were deposited on an aluminum stub and fastened with double-sided carbon tape. The excess powder was removed with compressed air before applying the carbon coating (Q150T 16,017, Quorum Technologies Ltd., Laughton, East Sussex, England). All powder samples were coated with carbon to improve electron conductivity and imaging. The particle morphology of each formulation was inspected by Field Emission Scanning Electron Microscope (EM JSM-7900F, JEOL Ltd., USA).

Powder Rheometer (FT4 Tester)

The bulk density (BD) and flow function coefficient (FFC) of the samples were measured using the powder rheometer Freeman Technology FT4 (Freeman Technology Ltd., UK). The BD, which is a conditioned bulk density, is highly repeatable and is an essential parameter to determine the amount of powder that can fit in a space, whereas the FFC represents powder flowability, both being the higher, the better. The 25 mm × 25 mL split vessel and 25 mm × 1 mL shear cell module were used for BD and FFC measurements, respectively.

The powder was consolidated at 9-kPa normal stress when FFC was measured [46]. Then, shear tests were performed at 3-, 4-, 5-, 6-, and 7-kPa normal stresses with recorded incipient failure shear stresses. The shear test findings were then put into the FT4 Data Analysis v4 program to calculate the FFC, which is a ratio of main principal stress to unconfined yield strength [72]. FFC < 2 means the powder is very cohesive and not flowing, 2 < FFC < 4 means the powder is cohesive, 4 < FFC < 10 means the powder is easy flowing, and FFC > 10 means the powder is free-flowing [72, 73]. It is worth noting that there are no physical distinctions when FFC is larger than 10.

A conditioning step was performed on the powder for both tests to standardize the powder's initial state. Each test was performed in triplicate, and the average is presented in Table III.

Dissolution Test

The amorphous form has greater solubility than the crystalline form. It is foreseen that ASDs can achieve supersaturation levels and have increased the bioavailability of poorly soluble drugs both *in vivo* and *in vitro* [74–76]. As a result, under supersaturating circumstances, the dissolution behavior of spray-dried ASDs and spray-dried AC with Neusilin® were examined. Dissolution experiments were carried out with powder containing an equivalent of 50 mg GF per 1000 mL DI water at 37 °C for each sample to explore supersaturating conditions (The solubility of GF in DI water at 37 °C is 14.2 mg/L.). The United States Pharmacopeia (USP) II paddle method was used to determine the drug release from ASDs or AC by a Distek 2100C dissolution tester (North Brunswick, NJ). A paddle speed of 50 rpm was maintained. During dissolution, the particles were thoroughly dispersed. Samples of 4 mL were obtained manually at 1, 2, 3, 4, 5, 10, 15, 20, and 30 min. Before UV spectroscopy tests, the solution was filtered with a 0.1-µm PVDF membrane-type syringe filter to remove any undissolved drug aggregates that could affect the results. The filtered samples were held at 37 °C and diluted in a 1 to 5 ratio with deionized water. The absorbance was measured by UV spectrophotometer (Agilent, Santa Clara, CA) at 291-nm wavelength. The API concentration was calculated using a pre-established calibration curve. The mean drug concentration and relative standard deviation were calculated using three replicates from each formulation.

Results and Discussion

Preparation of Spray-Dried ASDs, AC With Neusilin® UFL2, or US2

Spray-dried solid dispersions and composites with Neusilin® UFL2 or US2 were prepared using the material composition and process conditions mentioned in Tables I and II. To verify the successful transfer from crystalline to amorphous form, the physical state of drug molecules in as-received GF, spray-dried AC, and spray-dried ASDs was assessed by XRPD analysis. The results were presented in Fig. 2 and Table III. As-received GF showed multiple intense diffraction peaks in the XRPD pattern (Fig. 2) due to GF crystallinity. When comparing the spray-dried AC and spray-dried ASDs to their equivalent crystalline GF, no distinct peak was observed, as illustrated in Fig. 2. Halos were observed in the XRPD patterns for the ASD (sample #1) and both AC (samples #3, 6). As a result, the produced spray-dried ASDs and spray-dried AC were proven to be in the amorphous state after preparation, or their crystalline components were

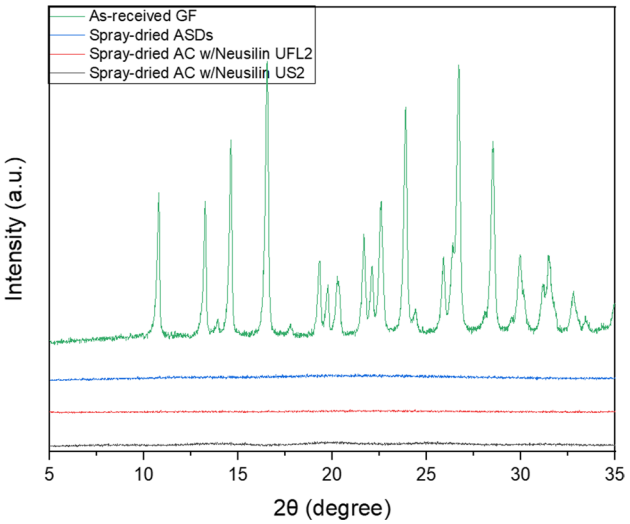

Fig. 2 XRD diffractograms for the as-received GF, spray-dried ASDs, and spray-dried AC with Neusilin.® US2 or UFL2

considerably below the XRPD method's detection limit. The result agreed with the findings observed by Sun et al. for GF-Neusilin® composites [53]. The drug loading of the spray-dried samples was calculated and found between 20 and 33% (w/w) (Table I), depending on the sample's composition.

Flow Property Improvement of Spray-Dried AC With Neusilin® UFL2 or US2

Powder flowability may be evaluated using Hausner's ratio, Carr's index, and shear test [77, 78]. Here, particle size, bulk density, and flow function coefficient via shear testing of as-received GF and different formulated spray-dried ASDs and ACs were measured using the FT4 powder rheometer. The particle sizes of the samples were measured as it impacts flowability. The bulk density, size, and flow function coefficient data were presented in Table III. Among six samples used in this research, three samples (#1: with ASDs, #3: with Neusilin® UFL2, and #6: with Neusilin® US2) were selected for flow property characterization, where sample 1 was the control, and samples 3 and 6 were chosen to observe the flow property difference due to the difference in the Neusilin® type as both had the same formulation compositions and drug loading.

According to Schulze [72], FFC values of powders may be classified into different regimes: FFC < 1: not flowing, 1 < FFC < 2: very cohesive, 2 < FFC < 4: cohesive, 4 < FFC < 10: easy flowing, and FFC > 10: free-flowing. The FFC of as-received GF was 3.16, which was in the cohesive regime and considered poor flowability [72, 79]. The spray-dried ASDs and AC had FFC of 7.35 and > 10, which indicated varying degrees of improvement in flowability compared to as-received GF. Generally, larger particles flowed better, and this had been reported in several publications [80, 81]. Comparing the particle size in Table III, as-received GF had the smallest particle sizes, d_{50} and d_{90} (11 µm and 21 µm, respectively). Spray-dried ASDs and AC with Neusilin® UFL2 had nearly the same d_{50} particle size (19 µm), whereas spray-dried AC with Neusilin® US2 had a d_{50} particle size (36 µm). Based on their particle sizes, it was reasonable that the as-received GF had the lowest FFC = 3.16 and corresponding poor flowability, whereas sample 6 had the highest flowability. It was noted that fine powders with a size smaller than 50 µm were cohesive and were usually unlikely to achieve the free-flowing category (FFC > 10) [82–84]. Therefore, as compared with the spray-dried ASD, the free-flowing property of spray-dried AC with Neusilin® represented a significant improvement in powder flowability.

It should be noted that UFL2 had very small sizes, d_{50} and d_{90}, 3 and 10 µm, respectively [55]. Due to the small size, larger surface area, and high adsorption capacity, most UFL2 was embedded into the final particles or covered by other excipients. Therefore, the particle sizes of AC with Neusilin® UFL2 showed little difference with ASDs. Unlike UFL2, US2 had a comparatively large particle size, and the d_{50} was 105 µm. However, it was surprising that the size of spray-dried AC with Neusilin® US2 was much smaller than that of US2. One of the reasons for this phenomenon may be the breakage of US2 during the atomization process in the spray drier [85]. When the fed solution was pumped into the spray drier, high air pressure (2 bar) was applied to spray the solution into droplets during the atomization step. The high pressure may have led to the collision or direct breakage of US2. Therefore, the spray-dried AC with Neusilin® US2 had a smaller size than US2 itself.

Spray-dried ASDs and spray-dried AC with Neusilin® UFL2 had similar mean particle sizes but different FFC. Hence, particle morphology was also investigated as besides the size, the morphology also impacted powder flowability [86]. To better understand the morphology of spray-dried powders, SEM images of as-received Neusilin®, spray-dried ASDs, and spray-dried AC with Neusilin® were shown in Fig. 3. For each sample, different images were shown at lower to higher magnifications. Figure 3a–c show that Neusilin® UFL2 and US2 particles had a highly rough and porous surface. Neusilin® UFL2 was composed of agglomerates of very fine particles, and Neusilin® US2 showed spherical appearance. Figure 3d–f present the spray-dried ASDs. The round-shaped ASD particles had a smooth surface with some minor concaves on the surface. In contrast, the spray-dried AC with Neusilin® UFL2 (Fig. 3g–i) or with US2 (Fig. 3j–l) had a much rougher surface. Figure 3m–o would be discussed in the next section. Overall, SEM images showed a variation in surface morphology, which contributed to better flowability [86]. This phenomenon strongly proved that the addition of Neusilin® could help to improve

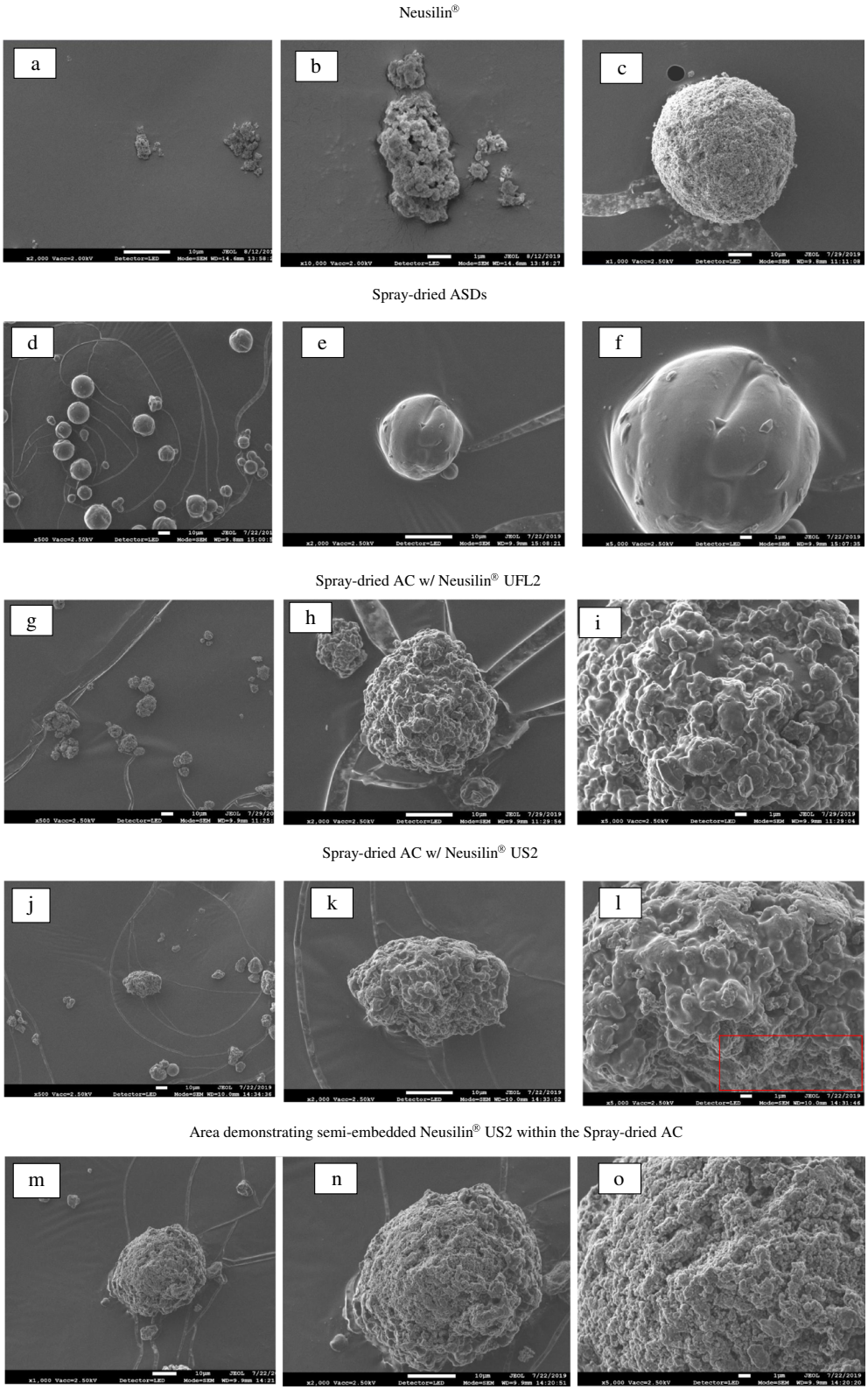

Fig. 3 SEM images of as-received Neusilin® **a** UFL2 at lower magnification, **b** UFL2 at higher magnification, **c** US2, **d–f** spray-dried ASDs, **g–i** spray-dried AC with Neusilin® UFL2, **j–l** spray-dried AC with Neusilin® US2, and **m–o** enlarged area demonstrating semi-embedded Neusilin® US2 within the spray-dried AC. For each case except pure Neusilin®, different images are shown at lower to higher magnification, respectively

powder flowability, and the spray-dried composite with Neusilin® could be free-flowing with such a fine size.

Comparing the bulk density of all samples (Table III), as-received GF had the lowest BD, whereas spray-dried ASD had the highest BD. GF had the smallest particle size among all of the samples. The higher cohesivity resulted in the strong interparticle force between smaller particles; ultimately, it led to lower bulk density. Hence, the powder may not pack itself in a denser state [77]. Compared with as-received GF, the bulk density of the spray-dried samples improved. Spray-dried ASDs showed a larger mean particle size than as-received GF. Previous contact models revealed that the larger particle sizes resulted in reduced cohesiveness [21]. Reduced cohesion would result in fragile structures that rapidly collapse in the powder bed and improve powder bed packing bringing higher bulk density [77]. Comparison between spray-dried AC showed that the powder with larger mean particle sizes had higher bulk density. Interestingly, spray-dried ASDs and spray-dried AC with Neusilin® UFL2 had similar particle sizes, but spray-dried AC with Neusilin® UFL2 had much a lower BD. This difference may have resulted from the porous structure of UFL2. The fed solution was absorbed and dried inside the pores of UFL2, which may lead to vacuum space inside the final particle [60, 87]. This behavior also explained why BD of spray-dried AC with Neusilin® US2 was lower than spray-dried ASDs.

Dissolution of Spray-Dried AC With Neusilin® UFL2 or US2 *vs.* ASDs

Polymer loading played a crucial influence on the supersaturation of GF in ASDs. To confirm the effect of Soluplus in the formulation, samples 2–4 were chosen for the dissolution test. Samples 2–4 had 3 g, 6 g, and 9 g Soluplus, respectively. As shown in Fig. 4, the amount of Soluplus was essential to maintain high supersaturation. With the increasing amount of Soluplus, spray-dried AC showed a higher drug release. The 6-g Soluplus formulation contained a different amount of UFL2 to examine the enhanced dissolution resulting from UFL2 rather than the impact stemming from Soluplus (Fig. 5). Formulations with or without Neusilin® showed almost similar drug concentration after 15 min. The main difference happened in the first 5 min, and sample no. 3 with 3 g UFL2 showed the fastest drug release. This result indicated that the porous structure of UFL2 with a higher surface area may contribute to drug dissolution [55]. However, the failure in higher supersaturation maintenance still left considerable room for improvement in dissolution. The size of UFL2 (3 µm) was much smaller than spray-dried AC with Neusilin® UFL2 (19 µm). It indicated that most UFL2 should be embedded inside spray-dried AC rather than be on the surface. If that indeed was the case, the surface morphology and visible features of these ACs should be more like spray-dried ASDs and not as-received UFL2. This was checked via observation of SEM images shown in Fig. 3b, f, and g–i. That may explain why sample no. 5 with 2 g UFL2 had a dissolution profile similar to the sample without Neusilin®. In Fig. 3l (spray-dried AC with Neusilin® US2), the top part showed a similar surface as spray-dried AC with Neusilin® UFL2, while the part marked with red box showed different morphology. For better comparison, Fig. 3m–o present the typical images where the rough surface of semi-embedded spray-dried AC with Neusilin® US2 was seen. Its morphology was discernibly different from the surface of Neusilin® UFL2, and more like Neusilin® US2. Such observations seemed to imply that Neusilin® US2 particles were only semi-embedded inside the spray-dried AC, and it was likely that most of the drug was absorbed into Neusilin® US2. Therefore, to reduce the tendency of Neusilin® to get embedded, the larger size Neusilin® US2 may be another choice. In Fig. 6, the dissolution of as-received GF, spray-dried ASDs, spray-dried AC with Neusilin® US2, and spray-dried AC with Neusilin® UFL2 were shown. Spray-dried ASDs and two spray-dried

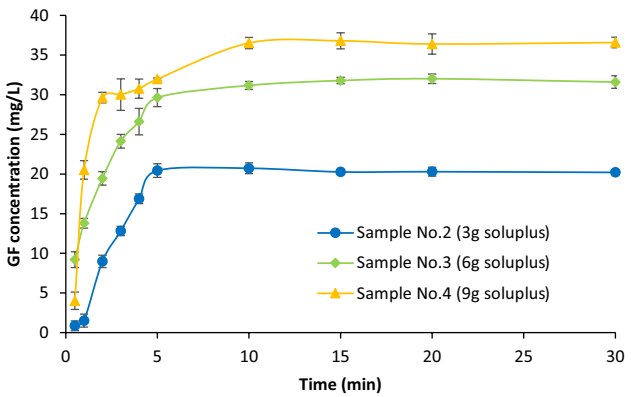

Fig. 4 Dissolution profiles of spray-dried AC with Neusilin® UFL2 with different Soluplus loading (3 g, 6 g, and 9 g)

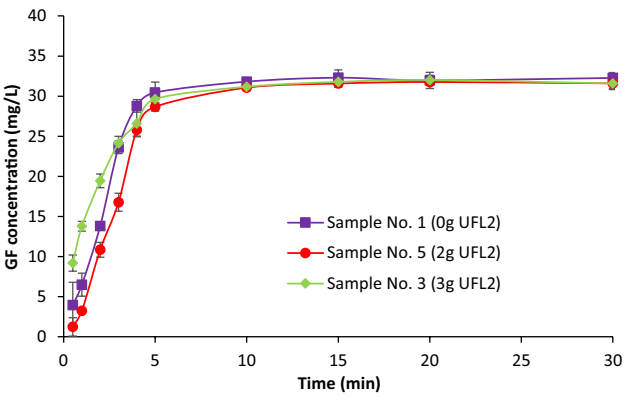

Fig. 5 Dissolution profiles of spray-dried AC having different UFL2 loading (3 g, 2 g, and 0 g)

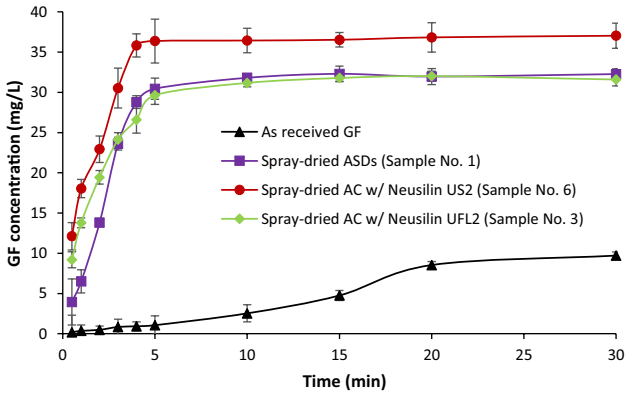

Fig. 6 Dissolution profiles comparison for as-received GF, spray-dried ASDs, spray-dried AC with Neusilin® UFL2, and spray-dried AC with Neusilin® US2. All samples contain 3 g GF, 0.15 g SDS, and 6 g Soluplus

ACs had achieved supersaturation, which was expected based on the XRD results discussed above. Spray-dried AC with Neusilin® US2 had the largest particle size (Table III), which was expected to have a lower total surface area and decreased dissolution rate. However, spray-dried AC with Neusilin® US2 represented a faster drug release rate and higher supersaturation. This indicated that the improvement in dissolution is not related to particle size but to the addition of Neusilin® US2. The existence of Neusilin® US2 on the surface may not only contribute to ASD formation but also inhibit recrystallization. These results confirmed the positive effect of Neusilin® in supersaturation maintenance and drug release, not to mention in improved flowability.

Conclusion

The findings reported above reveal that free-flowing spray-dried AC powders may be produced using Neusilin®. In addition, this spray-dried AC powder with Neusilin® US2 consists of a fully amorphous state of GF, achieving high supersaturation as well as faster drug release. The results demonstrated the positive impact of the amount of added Soluplus on supersaturation enhancement, albeit at the cost of decreased drug loading. For the fixed amount of Soluplus, the amount of Neusilin® UFL2 did not have any significant impact on the supersaturation level. However, as compared to UFL2, the same amount of Neusilin® US2 had a significant impact on enhanced supersaturation. Most interestingly, the spray-dried AC powders with Neusilin® US2 retained the advantage of a faster dissolution rate of relatively finer size (well below 50 µm), yet exhibited excellent flowability (FFC > 10, free-flowing), like powders having sizes over 100 µm (the spray-dried AC powders with Neusilin® UFL2 also achieved excellent flowability). Although the improved flowability is in part due to the increased size of US2-based AC powders, the role of Neusilin® in flowability improvement is clear considering that spray-dried AC with Neusilin® UFL2 had higher FFC than ASDs with a similar size. Although the addition of Neusilin® had a negative impact on reduced drug loading, the results showed that the benefits of including Neusilin® such as improved flowability, bulk density, and dissolution rate could outweigh the loss of drug loading.

Acknowledgements The authors are grateful to Freeman Technologies for supplying the FT4 Powder Rheometer and Fuji Chemicals for contributing the material samples for this study. The authors also thank for early discussions with Dr. Mahbubur Rahman related to the spray drying experiments and recent discussions with Dr. Guluzar Gorkem Buyukgoz about the characterization and interpretation of the results.

Author Contribution Zhixing Lin contributed to the experimental design, experimental work, and writing. Kai Zheng helped in the XRPD measurements and early experimental design. Dr. Rajesh Dave contributed to the supervision, securing of resources, experimental design, and revising of the manuscript. Dr. Mohammad Azad offered guidance and organization as well as editing of the manuscript.

Funding The National Science Foundation provided funding for this project under grants EEC-0540855 and IIP-1919037.

Data Availability The research data associated with this paper is available.

Declarations

Conflict of Interest The authors declare no competing interests.

References

1. Shah VP, Amidon GL, Amidon GL, Lennernas H, Shah VP, Crison JR. A theoretical basis for a biopharmaceutic drug classification: the correlation of *in vitro* drug product dissolution and *in vivo* bioavailability, Pharm Res 12, 413–420, 1995—Backstory of BCS. The AAPS J. 2014;16(5):894–8.
2. Salunke S, Brien FO, Tan DC, Harris D, Math MC, Ariën T, Klein S, Timpe C. Oral drug delivery strategies for development of poorly water soluble drugs in paediatric patient population. Adv Drug Deliv Rev. 2022;114507.
3. Kalepu S, Nekkanti V. Insoluble drug delivery strategies: review of recent advances and business prospects. Acta Pharmaceutica Sinica B. 2015;5(5):442–53.
4. PharmaCircle [Internet]. California (US): PharmaCircle (US); 2011 [updated 2011 March 28; cited 2022 Dec 15]. Available from: https://www.pharmacircle.com/presentations/Water_Insoluble_Strategies.pdf.
5. Rumondor AC, Dhareshwar SS, Kesisoglou F. Amorphous solid dispersions or prodrugs: complementary strategies to increase drug absorption. J Pharm Sci. 2016;105(9):2498–508.
6. Schultheiss N, Newman A. Pharmaceutical cocrystals and their physicochemical properties. Cryst Growth Des. 2009;9(6):2950–67.
7. Singhal D, Curatolo W. Drug polymorphism and dosage form design: a practical perspective. Adv Drug Deliv Rev. 2004;56(3):335–47.

8. Humberstone AJ, Charman WN. Lipid-based vehicles for the oral delivery of poorly water soluble drugs. Adv Drug Deliv Rev. 1997;25(1):103–28.
9. Zheng K, et al. Effect of particle size and polymer loading on dissolution behavior of amorphous griseofulvin powder. J Pharm Sci. 2019;108(1):234–42.
10. Singh A, Van Den Mooter G. Spray drying formulation of amorphous solid dispersions. Adv Drug Deliv Rev. 2016;100:27–50.
11. Serajuddin AT. Solid dispersion of poorly water-soluble drugs: early promises, subsequent problems, and recent breakthroughs. J Pharm Sci. 1999;88(10):1058–66.
12. Kesisoglou F, Panmai S, Wu Y. Nanosizing — oral formulation development and biopharmaceutical evaluation. Adv Drug Deliv Rev. 2007;59(7):631–44.
13. Brough C, Williams RO. Amorphous solid dispersions and nanocrystal technologies for poorly water-soluble drug delivery. Int J Pharm. 2013;453(1):157–66.
14. Adkins JC, Faulds D. Micronised fenofibrate. Drugs. 1997;54(4):615–33.
15. Atkinson R, et al. Effect of particle size on blood griseofulvin-levels in man. Nature. 1962;193(4815):588–9.
16 Englund D, Johansson E. Oral versus vaginal absorption in oestradiol in postmenopausal women. Effects of different particles sizes. Ups J Med Sci. 1981;86(3):297–307.
17. Gouthami KS, et al. Can crystal engineering be as beneficial as micronisation and overcome its pitfalls?: a case study with cilostazol. Int J Pharm. 2015;491(1–2):26–34.
18. de Villiers MM. Influence of agglomeration of cohesive particles on the dissolution behaviour of furosemide powder. Int J Pharm. 1996;136(1):175–9.
19. Huang Z, et al. Improved blend and tablet properties of fine pharmaceutical powders via dry particle coating. Int J Pharm. 2015;478(2):447–55.
20. Kunnath K, et al. Assessing predictability of packing porosity and bulk density enhancements after dry coating of pharmaceutical powders. Powder Technol. 2021;377:709–22.
21. Chen Y, et al. Fluidization of coated group C powders. AIChE J. 2008;54(1):104–21.
22. Jallo LJ, et al. Prediction of inter-particle adhesion force from surface energy and surface roughness. J Adhes Sci Technol. 2011;25(4–5):367–84.
23. Enstad G. Segregation of powders-mechanisms, processes and counteraction. In: Handbook of Powder Technology. Elsevier; 2001. p. 589–602.
24. Vasconcelos T, Sarmento B, Costa P. Solid dispersions as strategy to improve oral bioavailability of poor water soluble drugs. Drug Discovery Today. 2007;12(23–24):1068–75.
25. Rahman M, et al. Hybrid nanocrystal–amorphous solid dispersions (HyNASDs) as alternative to ASDs for enhanced release of BCS Class II drugs. Eur J Pharm Biopharm. 2019;145:12–26.
26. Bejan A. Fundamentals of exergy analysis, entropy generation minimization, and the generation of flow architecture. Intl J Of Energy Research. 2002;26(7).
27. Ziaee A, et al. Spray drying of pharmaceuticals and biopharmaceuticals: critical parameters and experimental process optimization approaches. Eur J Pharm Sci. 2019;127:300–18.
28. Bellinghausen R. Spray drying from yesterday to tomorrow: an industrial perspective. Drying Technol. 2019;37(5):612–22.
29. Lee SH, et al. Nano spray drying: a novel method for preparing protein nanoparticles for protein therapy. Int J Pharm. 2011;403(1–2):192–200.
30. Li X, et al. Nanoparticles by spray drying using innovative new technology: the Büchi Nano Spray Dryer B-90. J Control Release. 2010;147(2):304–10.
31. Rabbani NR, Seville PC. The influence of formulation components on the aerosolisation properties of spray-dried powders. J Control Release. 2005;110(1):130–40.
32. Schönfeld B, Westedt U, Wagner KG. Vacuum drum drying—a novel solvent-evaporation based technology to manufacture amorphous solid dispersions in comparison to spray drying and hot melt extrusion. Int J Pharm. 2021;596: 120233.
33. Chen XD, Mujumdar AS, editors. Drying technologies in food processing. 1st ed. Singapore: John Wiley & Sons; 2009.
34. Meng F, Dave V, Chauhan H. Qualitative and quantitative methods to determine miscibility in amorphous drug–polymer systems. Eur J Pharm Sci. 2015;77:106–11.
35. Islam MIU, Langrish TAG. The effect of different atomizing gases and drying media on the crystallization behavior of spray-dried powders. Drying Technol. 2010;28(9):1035–43.
36. Vehring R, Foss WR, Lechuga-Ballesteros D. Particle formation in spray drying. J Aerosol Sci. 2007;38(7):728–46.
37. Al-Khattawi A, Bayly A, Phillips A, Wilson D. The design and scale-up of spray dried particle delivery systems. Expert Opin Drug Deliv. 2018;15(1):47–63.
38. Barot B, et al. Development of directly compressible metformin hydrochloride by the spray-drying technique. Acta Pharm (Zagreb, Croatia). 2010;60(2):165–75.
39. Gonnissen Y, Remon JP, Vervaet C. Development of directly compressible powders via co-spray drying. Eur J Pharm Biopharm. 2007;67(1):220–6.
40. Limwong V, Sutanthavidul N, Kulvanich P. Spherical composite particles of rice starch and microcrystalline cellulose: a new coprocessed excipient for direct compression. AAPS PharmSciTech. 2004;5(2):e30-49.
41. Sosnik A, Seremeta KP. Advantages and challenges of the spray-drying technology for the production of pure drug particles and drug-loaded polymeric carriers. Adv Coll Interface Sci. 2015;223:40–54.
42. Lechuga-Ballesteros D, et al. Trileucine improves aerosol performance and stability of spray-dried powders for inhalation. J Pharm Sci. 2008;97(1):287–302.
43. Mangal S, et al. The role of physico-chemical and bulk characteristics of co-spray dried l-leucine and polyvinylpyrrolidone on glidant and binder properties in interactive mixtures. Int J Pharm. 2015;479(2):338–48.
44. Pinho LAG, et al. Improvements of theobromine pharmaceutical properties using solid dispersions prepared with newfound technologies. Chem Eng Res Des. 2018;132:1193–201.
45. Panda RR, Tiwary AK. Hot melt granulation: a facile approach for monolithic osmotic release tablets. Drug Dev Ind Pharm. 2012;38(4):447–61.
46. Davis MT, Potter CB, Walker GM. Downstream processing of a ternary amorphous solid dispersion: the impacts of spray drying and hot melt extrusion on powder flow, compression and dissolution. Int J Pharm. 2018;544(1):242–53.
47. Anagha B, et al. Bioavailability enhancement of poorly water-soluble drugs via nanocomposites: formulation–processing aspects and challenges. Pharmaceutics. 2018;10(3):86.
48. Gupta MK, et al. Enhanced drug dissolution and bulk properties of solid dispersions granulated with a surface adsorbent. Pharm Dev Technol. 2001;6(4):563–72.
49. Hong S, et al. High drug load, stable, manufacturable and bioavailable fenofibrate formulations in mesoporous silica: a comparison of spray drying versus solvent impregnation methods. Drug Delivery. 2016;23(1):316–27.
50. Augustijns P, Brewster ME. Supersaturating drug delivery systems: fast is not necessarily good enough. J Pharm Sci. 2012;101(1):7–9.
51. Surwase SA, et al. Polymer incorporation method affects the physical stability of amorphous indomethacin in aqueous suspension. Eur J Pharm Biopharm. 2015;96:32–43.
52. Azad M, et al. Fast dissolution of poorly water soluble drugs from fluidized bed coated nanocomposites: impact of carrier size. Int J Pharm. 2016;513(1–2):319–31.

53. Sun W-J, Aburub A, Sun CC. A mesoporous silica based platform to enable tablet formulations of low dose drugs by direct compression. Int J Pharm. 2018;539(1–2):184–9.
54. Sun W-J, Aburub A, Sun CC. Particle engineering for enabling a formulation platform suitable for manufacturing low-dose tablets by direct compression. J Pharm Sci. 2017;106(7):1772–7.
55. Azad M, Moreno J, Davé R. Stable and fast-dissolving amorphous drug composites preparation via impregnation of Neusilin® UFL2. J Pharm Sci. 2018;107(1):170–82.
56. Maclean J, et al. Manufacture and performance evaluation of a stable amorphous complex of an acidic drug molecule and neusilin. J Pharm Sci. 2011;100(8):3332–44.
57. Gupta MK, Vanwert A, Bogner RH. Formation of physically stable amorphous drugs by milling with Neusilin. J Pharm Sci. 2003;92(3):536–51.
58. Bahl D, Bogner RH. Amorphization of indomethacin by co-grinding with Neusilin US2: amorphization kinetics, physical stability and mechanism. Pharm Res. 2006;23(10):2317–25.
59. Knapik J, et al. Stabilization of the amorphous ezetimibe drug by confining its dimension. Mol Pharm. 2016;13(4):1308–16.
60. Allgeier MC, et al. Isolation and physical property optimization of an amorphous drug substance utilizing a high surface area magnesium aluminometasilicate (Neusilin® US2). J Pharm Sci. 2016;105(10):3105–14.
61. Grobelny P, et al. Amorphization of itraconazole by inorganic pharmaceutical excipients: comparison of excipients and processing methods. Pharm Dev Technol. 2015;20(1):118–27.
62. Rahman M, et al. Spray-dried amorphous solid dispersions of griseofulvin in HPC/Soluplus/SDS: elucidating the multifaceted impact of sds as a minor component. Pharmaceutics. 2020;12(3):197.
63. Ha E-S, et al. Preparation and evaluation of solid dispersion of atorvastatin calcium with Soluplus® by spray drying technique. Chem Pharm Bull. 2014;62(6):545–51.
64. Linn M, Collnot EM, Djuric D, Hempel K, Fabian E, Kolter K, Lehr CM. Soluplus® as an effective absorption enhancer of poorly soluble drugs in vitro and in vivo. Eur J Pharm Sci. 2012;45(3):336–43.
65. Nagy ZK, et al. Comparison of electrospun and extruded soluplus®-based solid dosage forms of improved dissolution. J Pharm Sci. 2012;101(1):322–32.
66. Alshahrani SM, et al. Stability-enhanced hot-melt extruded amorphous solid dispersions via combinations of Soluplus® and HPMCAS-HF. AAPS PharmSciTech. 2015;16(4):824–34.
67. Vehring R. Pharmaceutical particle engineering via spray drying. Pharm Res. 2008;25(5):999–1022.
68. Baird JA, Van Eerdenbrugh B, Taylor LS. A classification system to assess the crystallization tendency of organic molecules from undercooled melts. J Pharm Sci. 2010;99(9):3787–806.
69. Rahman M, et al. Synergistic and antagonistic effects of various amphiphilic polymer combinations in enhancing griseofulvin release from ternary amorphous solid dispersions. Eur J Pharm Sci. 2020;150: 105354.
70. Zhang P, et al. Supersaturation of poorly soluble drugs induced by mesoporous magnesium carbonate. Eur J Pharm Sci. 2016;93:468–74.
71. Han X, et al. Passivation of high-surface-energy sites of milled ibuprofen crystals via dry coating for reduced cohesion and improved flowability. J Pharm Sci. 2013;102(7):2282–96.
72. Schulze D. Powders and bulk solids: behavior, characterization, storage and flow. Berlin: Springer; 2007.
73. Azad MA, et al. A compact, portable, re-configurable, and automated system for on-demand pharmaceutical tablet manufacturing. Int J Pharm. 2018;539(1–2):157–64.
74. Leuner C, Dressman J. Improving drug solubility for oral delivery using solid dispersions. Eur J Pharm Biopharm. 2000;50(1):47–60.
75. Knopp MM, et al. Effect of polymer type and drug dose on the *in vitro* and *in vivo* behavior of amorphous solid dispersions. Eur J Pharm Biopharm. 2016;105:106–14.
76. Forster A, Hempenstall J, Rades T. Characterization of glass solutions of poorly water-soluble drugs produced by melt extrusion with hydrophilic amorphous polymers. J Pharm Pharmacol. 2001;53(3):303–15.
77. Abdullah EC, Geldart D. The use of bulk density measurements as flowability indicators. Powder Technol. 1999;102(2):151–65.
78. Freeman R. Measuring the flow properties of consolidated, conditioned and aerated powders — a comparative study using a powder rheometer and a rotational shear cell. Powder Technol. 2007;174(1–2):25–33.
79. Knieke C, et al. Sub-100 micron fast dissolving nanocomposite drug powders. Powder Technol. 2015;271:49–60.
80. Muteki K, MacGregor JF. Multi-block PLS modeling for L-shape data structures with applications to mixture modeling. Chemom Intell Lab Syst. 2007;85(2):186–94.
81. Yu W, et al. Prediction of bulk powder flow performance using comprehensive particle size and particle shape distributions. J Pharm Sci. 2011;100(1):284–93.
82. Capece M, et al. Prediction of powder flow performance using a multi-component granular Bond number. Powder Technol. 2015;286:561–71.
83. Capece M, et al. On the relationship of inter-particle cohesiveness and bulk powder behavior: flowability of pharmaceutical powders. Int J Pharm. 2016;511(1):178–89.
84. Tay JYS, Liew CV, Heng PWS. Powder flow testing: judicious choice of test methods. AAPS PharmSciTech. 2017;18(5):1843–54.
85. Ali M, et al. Particle breakage in a scirocco disperser. Powder Technol. 2015;285:138–45.
86. Vivacqua V, López A, Hammond R, Ghadiri M. DEM analysis of the effect of particle shape, cohesion and strain rate on powder rheometry. Powder Technol. 2019;342:653–63.
87. Ruffel L, et al. Ibuprofen loading into mesoporous silica nanoparticles using Co-Spray drying: a multi-scale study. Microporous Mesoporous Mater. 2020;291: 109689.

Publisher's Note Springer Nature remains neutral with regard to jurisdictional claims in published maps and institutional affiliations.

Springer Nature or its licensor (e.g. a society or other partner) holds exclusive rights to this article under a publishing agreement with the author(s) or other rightsholder(s); author self-archiving of the accepted manuscript version of this article is solely governed by the terms of such publishing agreement and applicable law.